EXPERIMENTAL and MOLECULAR MEDICINE, Vol. 41, No. 2, 102-115, February 2009

Genetic and expression alterations in association with the sarcomatous change of cholangiocarcinoma cells

Hee-Jung Yoo[1], Bo-Ra Yun[1], Jung-Hee Kwon[2], Hyuk-Soo Ahn[1], Min-A Seol[1], Mi-Jin Lee,[1] Goung-Ran Yu[1], Hee-Chul Yu[3], BeeHak Hong[2], KwanYong Choi[2] and Dae-Ghon Kim[1,4]

[1]Division of Gastroenterology and Hepatology
Department of Internal Medicine
Institute for Medical Sciences
Chonbuk National University Medical School and Hospital
Jeonju 561-712, Korea
[2]Department of Life Sciences
Pohang University of Science and Technology
Pohang 790-784, Korea
[3]Department of General Surgery
Chonbuk National University Medical School and Hospital
Jeonju 561-712, Korea
[4]Corresponding author: Tel, 82-63-250-1681;
Fax, 82-63-254-1609; E-mail, daeghon@chonbuk.ac.kr
DOI 10.3858/emm.2009.41.2.013

Accepted 3 November 2008

Abbreviations: CC, cholangiocarcinoma; Dox, doxorubicin; EMT, epithelial mesenchymal transition; FDR, false discovery rate; *FHIT*, fragile histidine triad; KRTs, keratins; SAM, significance analysis of microarray

Abstract

Cholangiocarcinoma (CC) is an intrahepatic bile duct carcinoma with a high mortality rate and a poor prognosis. Sarcomatous change/epithelial mesenchymal transition (EMT) of CC frequently leads to aggressive intrahepatic spread and metastasis. The aim of this study was to identify the genetic alterations and gene expression pattern that might be associated with the sarcomatous change in CC. Previously, we established 4 human CC cell lines (SCK, JCK1, Cho-CK, and Choi-CK). In the present study, we characterized a typical sarcomatoid phenotype of SCK, and classified the other cell lines according to tumor cell differentiation (a poorly differentiated JCK, a moderately differentiated Cho-CK, and a well differentiated Choi-CK cells), both morphologically and immunocytologically. We further analyzed the genetic alterations of two tumor suppressor genes (*p53* and *FHIT*) and the expression of *Fas/FasL* gene, well known CC-related receptor and its ligand, in these four CC cell lines. The deletion mutation of *p53* was found in the sarcomatoid SCK cells. These cells expressed much less *Fas/FasL* mRNAs than did the other ordinary CC cells. We further characterize the gene expression pattern that is involved in the sarcomatous progression of CC, using cDNA microarrays that contained 18,688 genes. Comparison of the expression patterns between the sarcomatoid SCK cells and the differentiated Choi-CK cells enabled us to identify 260 genes and 247 genes that were significantly over-expressed and under-expressed, respectively. Northern blotting of the 14 randomly selected genes verified the microarray data, including the differential expressions of the *LGALS1*, *TGFBI*, *CES1*, *LDHB*, *UCHL1*, *ASPH*, *VDAC1*, *VIL2*, *CCND2*, *S100P*, *CALB1*, *MAL2*, *GPX1*, and *ANXA8* mRNAs. Immunohistochemistry also revealed in part the differential expressions of these gene proteins. These results suggest that those genetic and gene expression alterations may be relevant to the sarcomatous change/EMT in CC cells.

Keywords: cholangiocarcinoma; gene expression profiling; oligonucleotide array sequence analysis; sarcoma

Introduction

Cholangiocarcinomas (CC) are primary malignancies of the biliary tract, and patients with these tumors have a poor prognosis because it is difficult to make an early diagnosis and the standard therapy is not very effective (Ahrendt *et al*., 2001). Chronic biliary tract inflammation resulting from bacterial infection or parasitic infestation or from a chronic inflammatory disease such as primary sclerosing cholangitis predisposes a patient to the development of CC (Chang *et al*., 1983). Most hepatic tumors with sarcomatous features are sarcomatoid carcinomas, whereas true hepatic sarcomas are extremely rare tumors (Kakizoe *et al*., 1987). These sarcomatoid cells are the result of a reversal of differentiation of ordinary hepatocellular carcinoma cells or adenocarcinomatous CC cells (Oda *et al*., 1994). Such tumors are predominantly composed of spindle-cell, giant cells

and bizarre cells that express cytokeratins (KRTs) as an epithelial marker and vimentin as a mesenchymal marker. It has been suggested that this tumor has an epithelial origin and it is then transformed to the sarcomatous type. The incidence of sarcomatous change in CC is approximately 5%. However, patients with these tumors show aggressive intrahepatic spread of tumor and widespread metastasis, and they have a poorer prognosis than those patients with ordinary CC. Epithelial tumor cells lose their restriction during the last steps of tumorigenesis, concomitant with the loss of epithelial characteristics and the acquisition of motile behavior. These changes contribute to a transition from an epithelial morphology toward a more mesenchymal fibroblastic (sarcomatoid) phenotype, and this is referred to as epithelial to mesenchymal transition (EMT) (Boyer *et al*., 1997).

The molecular mechanism whereby cancer cells generate a cell-autonomous EMT-like process *via* oncogenic activation is still unclear. One approach to understanding how genetic and molecular changes can lead to EMT is to compare the gene expression between tumor cells with EMT and the paired tumor cells without EMT. cDNA microarray is a well established technique to perform large-scale surveys of the expression of genes and to identify candidate target genes. We previously established four distinct CC cell lines (SCK, JCK1, Cho-CK, and Choi-CK) and we analyzed their chromosomal aberrations by cross-species color banding (Kim *et al*., 2001). One of them (SCK) was derived from the sarcomatoid CC. In this study, we verified the grade of differentiation in the four cell lines using a xenotransplanted nude mice model and examined a typical sarcomatoid phenotype of SCK cells both morphologically and immunocytologically. We further analyzed the status of tumor

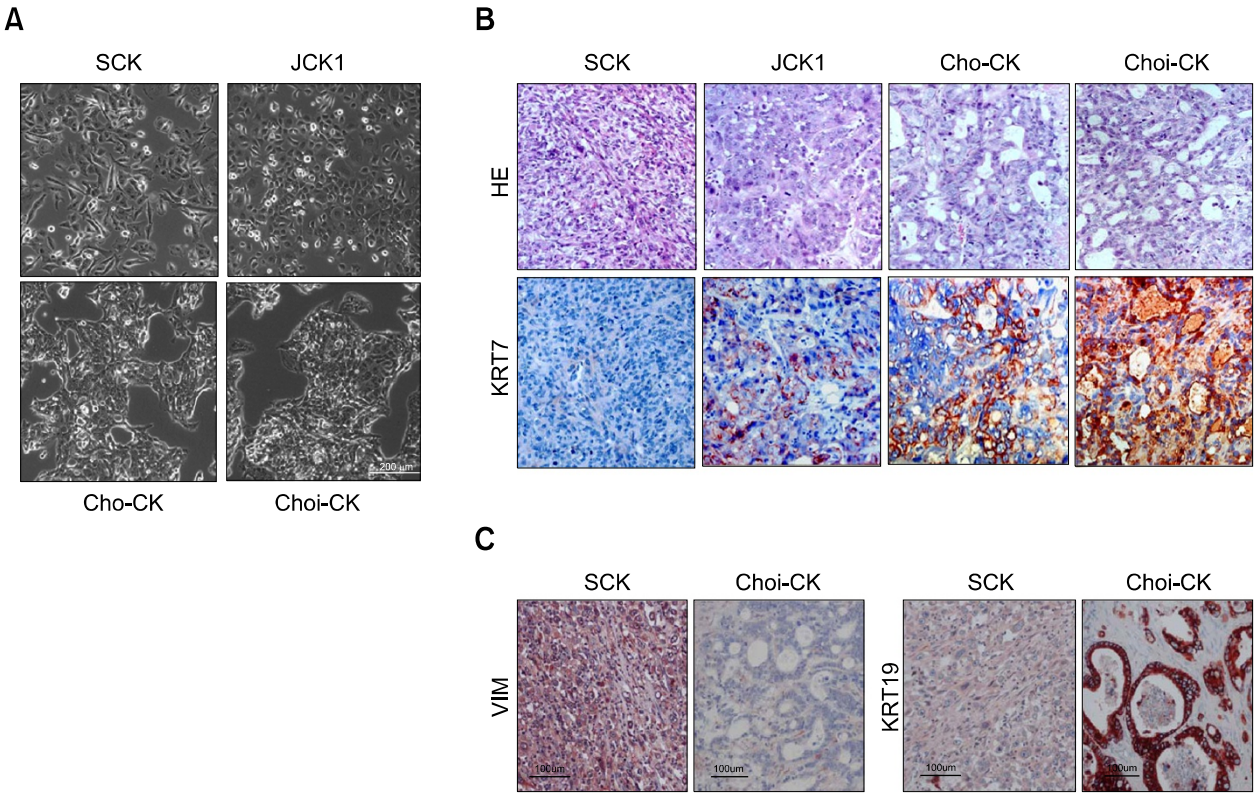

Figure 1. The morphological and immunohistochemical characteristics of the 4 CC cell lines. (A) Phase contrast images of the 4 CC cell lines that were monolayer-cultured in DMEM supplemented with 10% FBS and 1% antibiotics-antimycotics in a 5% CO_2-air conditioned 37°C incubator. (B) Histochemical findings of the xenotransplanted tumors derived from the 4 CC cell lines (SCK, JCK1, Cho-CK or Choi-CK). The anaplastic spindle cells with a fascicular arrangement in a xenotransplanted tumor derived from SCK cells. The poorly differentiated adenocarcinoma derived from the JCK1 cells. The moderately differentiated and the well differentiated adenocarcinomas derived from the Cho-CK and Choi-CK cells, respectively (H&E, ×100; upper panels). Immunohistochemistry (IHC) with an anti-KRT7 antibody stained for the xenotransplanted tumors derived from the 4 CC cell lines. SCK cell-derived tumor; most of the spindle cells were barely stained. IHC with anti-KRT7 antibody in the xenotransplanted tumor tissues, according to the tumor differentiation (lower panels). (C) Immunohistochemical staining of the original tumor tissues. Vimentin and KRT19 expressions were examined in the sarcomatoid (SCK) and the differentiated (Choi-CK) CC tissues, respectively.

suppressor genes, including the *p53* gene and the fragile histidine triad (*FHIT*) gene, and the expression of a well-known CC-related receptor and its ligand *Fas/Fas-ligand* (*FasL*) in the sarcomatous CC cell line as well as in other carcinomatous CC cell lines. In addition, we used cDNA microarrays to investigate the genes that are associated with EMT in CC. We found up- or down-regulated genes in the sarcomatous SCK cells, as compared with the differentiated Choi-CK cells. The genes identified or characterized through this approach are potential candidates for those genes involved in the cancer metastasis and invasiveness of CC.

Results

The histology and immunohistochemistry of the xenoplanted tumors

The SCK, JCK and Cho-CK cells were originally derived from a peripheral type of intrahepatic CC. The Choi-CK cells were cultured from a hilar type of infiltrative CC. The SCK cells showed the spindle- shaped (fibroblastoid) morphology and loose cell- cell adhesion. In contrast, the Cho-CK and Choi- CK cells showed the polygonal and epitheloid morphology, and tight cell-cell adhesion. The JCK1 cells showed the intermediate type of morphology between the SCK and Cho-CK cells (Figure 1A). All four CC lines were tumorigenic in nude mice. Following subcutaneous injection of tumor-cell suspensions into the nude mice, the resulting tumors reached diameters of 1 cm within 3 months. The histology of the tumors growing in the nude mice was similar to that of the original tumors. The xenoplanted SCK cell tumors were mainly composed of anaplastic spindle cells with a fascicular arrangement, and these findings were compatible with the characteristics of sarcomatoid adenocarcinoma. The xenotransplanted JCK1 cell tumors were poorly differentiated adenocarcinomas that consisted of nested large anaplastic cells with sparse glandular differentiation. The xenotransplanted Choi-CK or Cho-CK cell tumors revealed well- and moderately-differentiated adenocarcinomas, respectively, and these formed glandular structures (Figure 1B). A summary of the immunohistochemical results is shown in Table 1. The tumors originating from the JCK1, Cho-CK or Choi-CK cells showed positive reactions for KRT7 and for KRT19, which are well-known markers of bile duct cells, and they were also positive for EMA. The sarcomatoid carcinoma SCK cell tumors were barely positive for KRT7/19, they were strongly positive for vimentin and they had a luminal staining pattern for CEA at a few abortive glandular luminal borders. Immunoreactivity for EMA was positive in the primary SCK tumors, but this was negative in the xenoplanted tumors from the SCK cells. All the other markers of hepatocellular carcinoma that were tested were negative for all 4 types of tumors.

Table 1. The expression patterns of marker proteins by immunohistochemical staining.

Antigen	SCK	JCK1	Cho-CK	Choi-CK
KRT7	-	+/-	+	++
KRT19	+/-	+	+	+/-
KRT20	-	-	-	-
CEA	+/-	+/-	+	++
EMA	- (+)*	+	+	+
VIM	++	-	-	-
AFP	-	-	-	-
Albumin	-	-	-	-
Fibrinogen	-	-	-	-

-, $>$ 95% of the cells could not be determined as positive; +/-, the cells are focally positive between 5% and 24%; +, the percentage of cells determined as positive is from 25% up to 75%; ++, $>$ 75% of the cells are positive with clearly distinguishable strength. *The immunoreactivity for KRT7 or EMA was positive in the primary tumors, but it was negative in the xenotransplanted tumors (KRT, keratin; CEA, carcinoembryonic antigen; EMA, epithelial membrane antigen; VIM, vimentin; AFP, alpha-fetoprotein).

p53 mutations

We examined the p53 protein expression by immunoblot analysis in the four CC cell lines and we found that the Cho-CK and Choi-CK cells strongly expressed p53 protein, but the SCK and JCK1 cells weakly expressed p53 protein (Figure 2A). Particularly, the size of the p53 protein expression of the JCK1 cells was smaller than that of other CC cells on PAGE electrophoresis. The p21, which is downstream from the p53, was detected in the Choi-CK cells, but p21 was weakly expressed in the SCK and Cho-CK cells. The JCK1 cells did not show a p21 expression. To determine the p53 function, we treated the cells with the p53-inducing agent doxorubicin (Dox, 0.2 μg/ml). Dox efficiently induced a p53 expression in the SCK, Cho-CK, and Choi CK cells in a time dependent manner, but it did not in the JCK1 cells. Induction of the p53 expression was accompanied by the downstream p21 expression. These results suggested that the SCK, Cho-CK, and Choi-CK cells have the functional p53, but the JCK1 cells have nonfunctional p53. Next we checked the *p53* mutation by genomic DNA sequencing and the cDNA sequencing method (Table 2). SCK showed a deletion mutation of 24 bp of codon 262 to 269

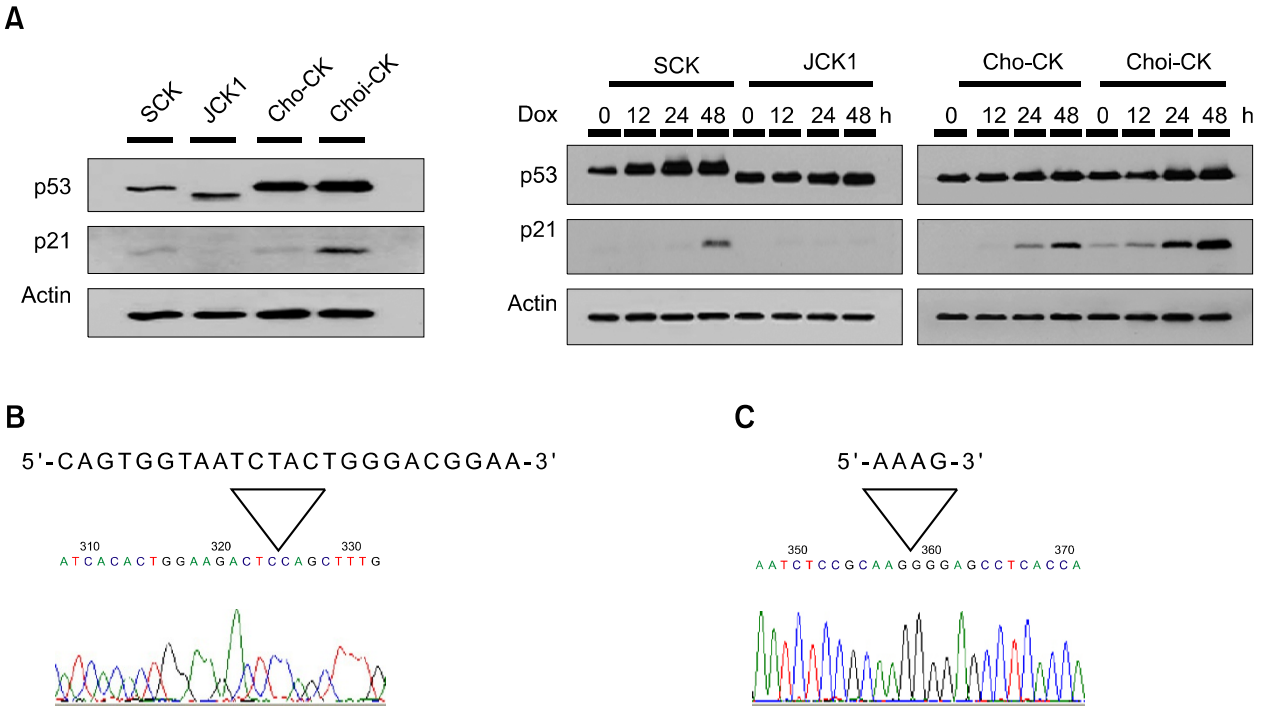

Figure 2. The functional status and the mutation analyses of the *p53* in the 4 CC cell lines. (A) The p53 expression was analyzed by Western blot analysis. Thirty μg of extracted proteins were resolved by 12% SDS-PAGE and then they were transferred to the membrane. The blots were probed with anti-p53 (DO-1) or anti-p21 (C-19) antibody, and then they were stripped and reprobed with a monoclonal antibody to actin as a loading control. To activate the *p53* gene expression, the cells were treated with 0.2 μg/ml doxorubicin (Dox) for the indicated time intervals. Thirty μg of the cell lysates were processed for Western blot analysis (right two panels). (B) The sequencing profiles show a deletion of 24 bp in codon 262-269 (nt 977-1000, NM_000546.4) spanning exon 7 and exon 8 without a frame shift in the *p53* gene of the SCK cells. (C) A deletion of 4 bp in codon 292-293 of exon 8 (nt 1071-1074, NM_000546.4) with a frame shift in the *p53* gene of the JCK cells. (D) The premature termination and altered N-terminal amino acids (bold and underlined) by the frame shift in the *p53* gene of the JCK cells.

Table 2. Somatic mutation of *p53* in the human intrahepatic cholangiocarcinoma cell lines.

Cell line	Polymorphism	Point mutation	Frame shift	Deletion	Premature termination
SCK	CCC (Pro) > CGC (Arg); codon 72 of exon 4	-	-	24 bp; codon 262 -269 of exon 8	-
JCK1	-	-	+	4bp; codon 292 -293 of exon 8	+
Cho-CK	-	GTG (Val) > GCG (Ala) Codon 143 of exon 5	-	-	-
Choi-CK	-	ATG (Met) > GTG (Val); codon 169 of exon 5 CGT (Arg) > TGT (Cys) Condon 273 of exon 8	-	-	-

(NM_000546.4) without a frame shift. In contrast, the JCK1 cells showed a deletion mutation of 4 bp in codon 292 to 293 with a frame shift and premature termination (Figure 2B and C). The JCK1 cells also revealed the mutant *p53* that consisted of 342 amino acids, which is smaller than the wild-type *p53* that consisted of 393 amino acids (Figure 2D). In addition, Cho-CK cells showed a point mutations in codon 143, while Choi-CK cells revealed two point mutations in codon 169 and 273 of *p53*, respectively.

The expressions of the *FHIT* gene and *Fas/FasL* mRNA

All four CC cell lines expressed the *FHIT* gene transcripts. A PCR product of 707 bp (using primers 5U1 and 3D1), which corresponded to the expected size of the *FHIT* RT-PCR product (Ohta *et al*., 1996), was observed in the JCK1 and Cho-CK cells. However, the SCK cells displayed normal and aberrant *FHIT* gene transcripts, implying that the normal and abnormal alleles function together. The Choi-CK cells showed an aberrant *FHIT* transcript (Figure 3A). The second set of primers (MUR5 and RP2) amplifies a fragment of *FHIT* cDNA that is identical to, but 40 bp longer, than the fragment generated by 5U1 and 3D1. Next, we determined whether the altered expression of the apoptosis-related genes such as Fas/FasL is associated with the tumor progression of CC. RT-PCR analysis revealed that all 4 CC cell lines expressed *Fas* and *FasL*, although their expression levels varied among the different cell lines. The SCK cells had lower expression levels of *Fas/FasL* mRNA, which was consistent with the previous report (Shimonishi *et al*., 2000). In contrast, the JCK1, Choi-CK and Cho-CK cells revealed higher expression levels of Fas/FasL mRNA (Figure 3B).

The differential expression of mRNAs in the sarcomatoid CC cells

To identify the distinct genes related to sarcomatous events, we performed gene expression profiling with using cDNA microarrays. The gene expression changes were mainly monitored using the high density microarrays with 14,080 (14k) cDNAs. Three separate mRNA isolations were obtained from each cell line and pair-wise hybridizations were then performed three times. Three independent hybridizations were repeated for the dye-swap experiments. The hybridizations were scanned and quantitative information was obtained for each hybridization. In order to search for the genes with significant differences in expression between the sarcomatous CC and the well differentiated CC cells, we performed the SAM one-class test (Figure 4A and B). Starting with their expression values from the 14k dataset (14,077 genes), this approach resulted in a list of 456 clones (244 up-regulated and 212 down-regulated), using a significance threshold that was expected to produce fewer than 10 false positives. A similar procedure was applied to the 4.6k dataset (4,414 genes) with fewer than 3 expected false positives. Additional 51 clones (16 up-regulated and 35 down-regulated) were selected. From these lists, we report in Table 3 only on those genes that were

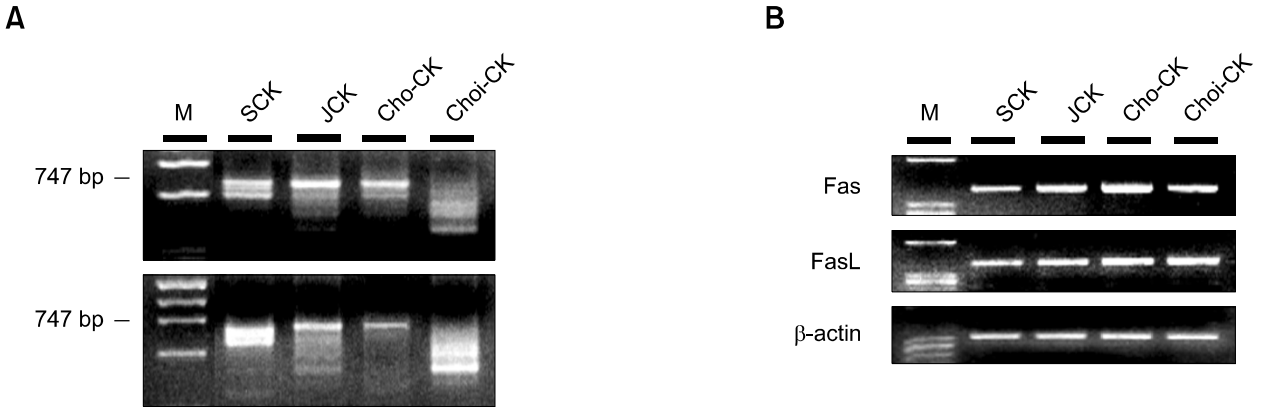

Figure 3. Genetic alterations of *FHIT* and *Fas/FasL* in the CC cells. (A) RT-PCR analysis of the *FHIT* gene product in the 4 CC cell lines with using nested PCR. The total RNA isolated from the cells was subjected to RT-PCR. Inner primers 5U1 and 3D1 were used (upper). Inner primers MUR5 and RP2 were used (lower). The PCR products were separated on 2% agarose gels. Arrow, the 707 bp or 747 bp *FHIT* gene product. Lane M, molecular weight markers. (B) Semiquantitative PCR analysis of the *Fas/FasL* mRNA expression. The total RNA was extracted from the CC cell lines. The *Fas/FasL* mRNA expression was analyzed by reverse-transcriptase PCR with using primers for *Fas/FasL* and for *β-actin* as an internal control, as described in the Methods section.

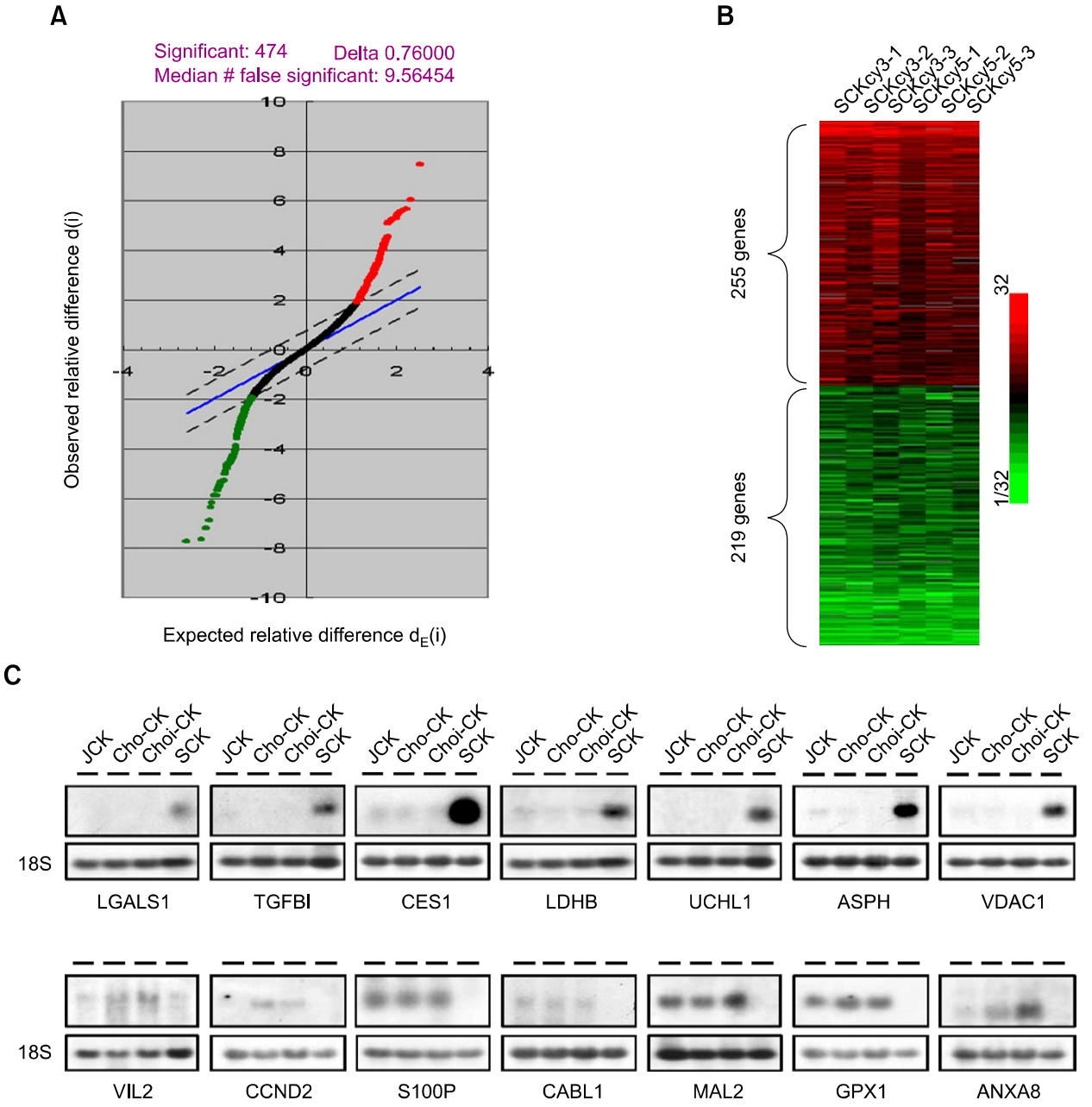

Figure 4. Pair wise analysis by a modified *t*-test of SAM and the validation of the cDNA microarray data. (A) The scatter plot of the observed relative difference (*di*) versus the expected relative difference $d_E(j)$. The solid line indicates the line for $d(i) = d_E(j)$, where the observed relative difference is identical to the expected relative difference. The dashed lines are drawn at a distance $\Delta = 0.758$ from the solid line. The 474 potentially significant genes for $\Delta = 0.758$ are indicated by red circles (255 up-regulated genes) and green circles (219 down-regulated genes) from the 14k dataset (14,077 genes). (B) The raw expression values ($\log_2$) of the 474 differentially expressed genes for the SCK cells, as compared to the control for the Choi-CK cells, are shown rank-ordered according to the fold change score. The triplicate expression ratios (the Cy5/Cy3 ratio) between the experimental samples (SCKCy5-1, -2, and -3) and the reference (Choi-CKCy3-1, -2, and -3) were repeated after swapping dye (SCKCy3-1, -2, and -3 *versus* Choi-CKCy5-1, -2, and -1). (C) Northern blot analysis of the *LGALS1*, *TGFBI*, *CES1*, *LDHB*, *UCHL1*, *ASPH*, *VDAC1*, *VIL2*, *CCND2*, *S100P*, *CALB1*, *MAL2*, *GPX1* and *ANXA8* gene expressions for the validation of the cDNA microarray data. The total RNA extracts from the JCK, Cho-CK, Choi-CK and SCK cells were fractionated by electrophoresis on 1% agarose gels that contained formaldehyde, and the proteins were then transferred to membranes. The blots were hybridized overnight with 2×10^6 cpm/ml of each cDNA probe labeled with [P^{32}]dCTP (NEN) by randompriming; they were then washed and next exposed to X-Omat AR film (Kodak) at -70°C. The blot was stripped and subsequently rehybridized with a probe for *18S* cDNA as a loading control (*lower*).

Table 3. The genes that are differentially expressed between the sarcomatoid (SCK) and the differentiated (Choi-CK) CC cells.

A. The differentially up-regulated genes in the sarcomatoid CC cells.

Function	Unigene ID	Unigene No	Annotation	Symbol	Fold change
Cell adhesion	240388	Hs.445351	Galectin-1	*LGALS1*	10.3
	131112	Hs.1908	Serglycin	*SRGN*	5.2
	143717	Hs.106880	Bystin-like	*BYSL*	4.8
	131973	Hs.6838	Rho family GTPase 3	*RND3*	4.7
	2481209	Hs.650585	Laminin, beta 1	*LAMB1*	4.2
	139586	Hs.73793	Vascular endothelial growth factor A	*VEGFA*	4.2
	1205348	Hs.531081	Lectin, galactoside-binding, soluble, 3 (galectin 3)	*LGALS3*	4.1
Cytoskeletal structure	2224039	Hs.642813	Vimentin	*VIM*	14.8
Growth regulation	619193	Hs.450230	Insulin-like growth factor-binding protein-3 gene	*IGFBP3*	7.4
	158415	Hs.173894	Macrophage-specific colony-stimulating factor	*CSF-1*	6.6
	198057	Hs.118787	Transforming growth factor, beta-induced, 68 kD	*TGFBI*	5.8
Metabolism	1841001	Hs.558865	Carboxylesterase 1	*CES1*	10.6
	241186	Hs.446	Lactate dehydrogenase B	*LDHB*	5.1
	172529	Hs.268849	Glyoxalase I	*GLO1*	4.1
Transcription	140374	Hs.79353	Transcription factor Dp-1	*TFDP1*	5.9
	1953698	Hs.584909	SCAN domain-containing 1	*SCAND1*	4.9
	150816	Hs.14453	Interferon regulatory factor 8	*IRF8*	4.4
Protein processing	909478	Hs.518731	Ubiquitin carboxyl-terminal esterase L1	*UCHL1*	23.2
	3525600	Hs.714780	Transducer of ERBB2, 1	*TOB1*	5.8
Miscellaneous	703399	Hs.488240	Uridine phosphorylase	*UP*	12.4
	092009	Hs.622998	Aspartate beta-hydroxylase, transcript variant 3	*ASPH*	11
	136757	Hs.40499	Dickkopf (Xenopus laevis) homolog 1	*DKK1*	10.7
	136499	Hs.37107	Melanoma antigen, family A, 4	*MAGEA4*	8.5
	162861	Hs.203206	Exportin 5 mRNA	*XPO5*	6.2
	136473	Hs.6120	Zinc finger, AN1-type domain 3	*ZFAND3*	5.7
	3525587	Hs.714767	Golgi reassembly stacking protein 1	*GORASP1*	5.3
	2065460	Hs.596449	Serpin peptidase inhibitor, clade H (heat shock protein 47), member 1	*SERPINH1*	4.8
	716538	Hs.501379	DEAD/H (Asp-Glu-Ala-Asp/His) box polypeptide 32	*DHX32*	4.7
	1086100	Hs.525899	Prickle homolog 4 (Drosophila)	*PRICKLE4*	4.7
	231694	Hs.436657	Clusterin	*CLU*	4.6
	2976618	Hs.696013	H2A histone family, member Y	*H2AFY*	4.5
	154270	Hs.153952	5' nucleotidase (CD73)	*NT5*	4.3
	183662	Hs.311190	Mitochondrial ribosomal protein L14	*MRPL14*	4.2
	910067	Hs.519320	Voltage-dependent anion channel 1	*VDAC1*	4.2
Unknown	715671	Hs.500	ycomb group ring finger 5	*PCGF5*	8.4
	137156	Hs.44098	Hypothetical gene supported by BX647608	*LOC399959*	8.1
	3525613	Hs.714793	ESTs		7.9
	2092009	Hs.622998	ESTs		7.2
	135738	Hs.30026	cDNA FLJ77664 complete cds	*FLJ77664*	6.5
	198869	Hs.370781	Pyridoxal-dependent decarboxylase domain containing 1	*PDXDC1*	4.9
	13090	Hs.1048	KIT ligand	*KITLG*	4.79
	1782987	Hs.567498	Chromosome 4 open reading frame 18	*C4orf18*	4.6

The genes up-regulated by more than 4-fold were selected by SAM analysis with an FDR up to 0.02. Unigene ID and Unigene No were based on the database of UniGene Build #215.

B. The differentially down-regulated genes in the sarcomatoid CC cells.

Function	Unigene ID	Unigene No	Annotation	Symbol	Fold change
Cytoskeletal structure	219875	Hs.406013	Keratin 18	*KRT18*	-10.6
	170416	Hs.253903	Stomatin	*STOM*	-9.1
	709078	Hs.493919	Myelin protien zero-like 1	*MPZL1*	-9.1
	221823	Hs.411501	Keratin 7	*KRT7*	-6.3
	2723698	Hs.654380	Keratin 14 (epidermolysis bullosa simplex, Dowling-Meara, Koebner)	*KRT14*	-6
	157619	Hs.170473	Pleckstrin 2 (mouse) homolog	*PLEK2*	-5.5
	1293157	Hs.533782	Keratin 8	*KRT8*	-5.4
	2723888	Hs.654570	Keratin 15	*KRT15*	-5.3
	2723886	Hs.654568	Keratin 19	*KRT19*	-5.1
	909782	Hs.519035	Ladinin 1	*LAD1*	-4.5
	702186	Hs.487027	Villin 2 (ezrin)	*VIL2*	-4
Cell growth	703452	Hs.488293	Epidermal growth factor receptor (avian erythroblastic leukemia viral (v-erb-b) oncogene homolog)	*EGFR*	-10.9
	145212	Hs.118110	Bone marrow stromal cell antigen 2	*BST2*	-9.2
	201376	Hs.376071	Cyclin D2	*CCND2*	-7.3
	173112	Hs.270833	Amphiregulin (schwannoma-derived growth factor)	*AREG*	-6.2
Cell signaling	907411	Hs.516664	Ephrin-A1	*EFNA1*	-9
	172401	Hs.268177	Phospholipase C, gamma 1 (formerly subtype 148)	*PLCG1*	-4.5
	14403	Hs.110642	EST		-4.1
	627377	Hs.458414	Interferon induced transmembrane protein 1 (9-27)	*IFITM1*	-4
Transcription	146283	Hs.122523	Staphylococcal nuclease and tudor domain containing 1	*SND1*	-12
	2724606	Hs.655288	Male-specific lethal-3 (Drosophila)-like 1	*MSL3L1*	-5.3
	13102	Hs.1545	Caudal type homeo box transcription factor 1	*CDX1*	-4.7
	716182	Hs.501023	MAX-interacting protein 1	*MXI1*	-4.3
Calcium binding	131328	Hs.2962	S100 calcium-binding protein P	*S100P*	-17.1
	139098	Hs.65425	Calbindin 1, (28 kD) (CALB1)	*CALB1*	-4.1
Protein biosynthesis	1955212	Hs.586423	Eukaryotic translation elongation factor 1, alpha 1	*EEF1A1*	-9.4
	219562	Hs.405590	Eukaryotic translation initiation factor 3, subunit 6 (48 kD)	*EIF3S6*	-5.5
Major histocompability antigen	2723722	Hs.654404	Major histocompatibility complex, class I, C	*HLA-C*	-8.2
	140173	Hs.77961	Major histocompatibility complex, class I, B	*HLA-B*	-8
	910719	Hs.519972	Major histocompatibility complex, class I, F	*HLA-F*	-7
Miscellaneous	2723831	Hs.58247	Protease, serine, 3	*PRSS3*	-22.2
	198836	Hs.370725	Oxysterol binding protein-like 1A	*OSBPL1A*	-15.4
	133582	Hs.16426	Podocalyxin-like	*PODXL*	-11.1
	162274	Hs.76550	Mal, T-cell differentiation protein 2	*MAL2*	-10.4
	131280	Hs.2704	Glutathione peroxidase 2 (gastrointestinal)	*GPX2*	-9.5
	139672	Hs.74471	Homo sapiens gap junction protein, alpha 1, 43 kD (connexin 43)	*GJA1*	-7.3
	3369927	Hs.714347	Vestigial like 3 (Drosophila)	*VGLL3*	-6.7
	142859	Hs.100686	Anterior gradient homolog 3 (Xenopus laevis)	*AGR3*	-6.6
	915027	Hs.524280	H2A histone family, member J	*H2AFJ*	-5.6
	3321528	Hs.709321	Interferon induced transmembrane protein 2 (1-8D)	*IFITM2*	-5.5
	220890	Hs.407995	Macrophage migration inhibitory factor	*MIF*	-5.1
	1281472	Hs.532634	Interferon, alpha-inducible protein 27	*IFI27*	-4.7
	132000	Hs.6980	Aldo-keto reductase family 7, member A3	*A AKR7A3*	-4.5
	154247	Hs.153768	Ribosomal RNA processing 9, small subunit (SSU) processome component, homolog (yeast)	*RRP9*	-4.3

B. Continued.

Function	Unigene ID	Unigene No	Annotation	Symbol	Fold change
	239804	Hs.444767	Kinesin family member 13B	*KIF13B*	-4.2
	907713	Hs.516966	BCL2-like 1	*BCL2L1*	-4.2
	1371620	Hs.535306	Annexin A8	*ANXA8*	-4.1
Unknown	1371620	Hs.535306	Hypothetical protein FLJ20171	*FLJ20171*	-9.3
	132620	Hs.10095	Similar to hCG2004878	*LOC729433*	-8.5
	156459	Hs.162757	Low density lipoprotein-related protein 1	*LRP1*	-5.5
	169386	Hs.177425	Discs, large (Drosophila) homolog-associated protein 4	*DLGAP4*	-5.4
	2728719	Hs.659401	cDNA FLJ34018 fis, clone FCBBF2002801		-5.2
	677500	Hs.462341	Myosin phosphatase Rho interacting protein	*MPRIP*	-5
	132883	Hs.12319	Amyotrophic lateral sclerosis 2 (juvenile) chromosome region, candidate 4	*ALS2CR4*	-4.5
	702630	Hs.487471	RNA binding motif protein 35A	*RBM35A*	-4.5

The genes down-regulated by more than 4-fold were selected by SAM analysis with an FDR up to 0.02. Unigene ID and Unigene No were based on the database of UniGene Build #215.

up- or down-regulated by more than 4-fold. The expression of 42 genes was enhanced at least 4-fold in the SCK cells, while that of 55 genes was reduced by 4-fold or more. The expression of vimentin showed the highest fold induction (24.7-fold). We also observed the up-regulation of genes that encode adhesion molecules, including *LGAL1*, *PRG1*, *BYSL*, *ARHE*, *LAMB1*, *VEGF* and *LGAL3*. Genes associated with cell growth regulation (*IGFBP3*, *CSF-1* and *TGFBI*) were also over- expressed in the SCK cells. In contrast, the expression of the *PRSS4* gene showed the largest decrease in expression (-22.2-fold). The down- regulated cytoskeletal structure genes included *KRT18*, *EPB72*, *MPZL1*, *KRT7*, *KRT14*, *PLEK2*, *KRT8*, *KRT15*, *KRT19*, *LAD1* and *VIL2* in the sarcomatous CC cells.

Verification of the cDNA microarray data

The preferential expression of VIM or CK7/19 in the SCK or Choi-CK cells, respectively, was confirmed by immunohistochemical staining, as is shown in Figure 1. Thus, to further validate the cDNA microarray data, 14 genes were randomly selected and these were examined by Northern blotting (Figure 4C). The *LGALS1*, *TGFBI*, *CES1*, *LDHB*, *UCHL1*, *ASPH* and *VDAC1* mRNAs were preferentially expressed in the SCK cells in accordance with the microarray results. The *VIL2*, *CCND2*, *S100P*, *CALB1*, *MAL2*, *GPX2* and *ANXA8* mRNAs were over-expressed in the carcinomatous CC cell lines, whereas their expressions were not detectable, or they were weak, in the sarcomatoid SCK cells, which was also consistent with the microarray data. Interestingly, the expression of *VIL2* and *ANXA8* mRNA decreased according to the degree of abnormal differentiation. Next, we immunohistochemically validated the expressions of four genes, *LDHB*, *UCHL1*, *S100P*, and *GPX1* in CC tissues with well, moderate, poor, or sarcomatous differentiation, respectively (Figure 5). The immunoreactivities of LDHB and UCHL1 were increased according to the degree of abnormal tumor differentiation. In contrast, the immunoreactivities of S100P and GPX1 were decreased according to the degree of abnormal tumor differentiation. These findings were consistent with the microarray data.

Discussion

The KRT profile of normal cells, from which tumor stem cells are generally retained during neoplastic transformation, can be used for differentiating hepatocellular carcinoma from CC (Wu *et al*., 1996). Thus, KRTs are a widely recognized tool for the phenotypic identification of hepatocytes (these are positive for KRT8 and KRT18) and bile-duct cells (these are positive for KRT7, KRT8, KRT18 and KRT19). However, this distinction is not applicable to all primary liver tumors and especially to mixed neoplasms, where the morphology and expression of different KRTs frequently overlap (Goodman *et al*., 1985). The combination of morphology and the expression of KRTs and albumin can reliably differentiate the majority of hepatocellular carcinomas and CC (D'Errico *et al*., 1996). Our data provide evidence that SCK cells are sarcomatous CC cells. Fortunately, the other 3 CC cell lines (JCK1, Cho-CK and Choi-CK cells) show different histological grades of differentiation, e.g., they are poorly, moderately and well differentiated phenotypes, respectively. Thus, we suggest that these cells are excellent models to investigate the

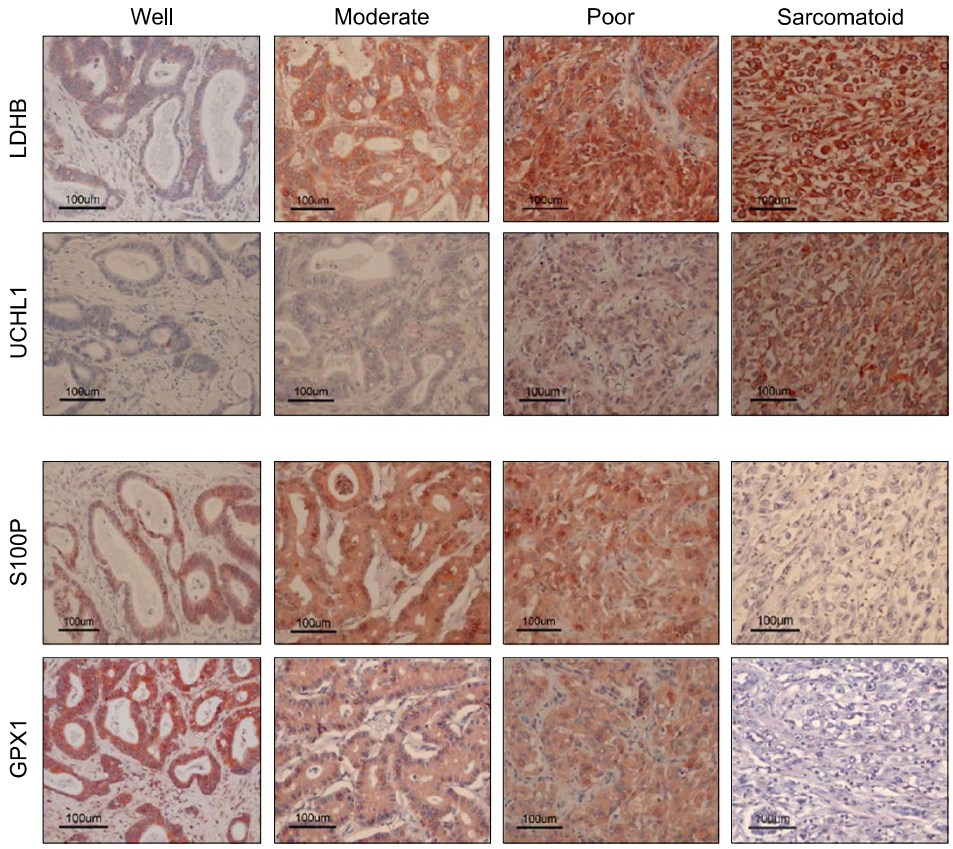

Figure 5. Immunohistochemical examination of the gene expressions in CC tissues with well, moderate, poor, or sarcomatous differentiation, respectively. The expressions of LDHB (A) and UCHL1 (B), S100P (C), and GPX1 (D) were increased or decreased according to the degree of abnormal tumor differentiation.

progression of CC.

The *p53* gene is one of the most frequently mutated genes in all types of cancers. Most *p53* mutations occur in exons 5-8 (Levine, 1992). However, mutations also occur at other sites as well. We extended the examination of the *p53* gene from exons 1 to 10. The deletion mutation of the p53 gene may be involved in the sarcomatous change or the tumor progression of CC cells. The *FHIT* gene was recently described as another candidate tumor suppressor gene that has been implicated in the development of various epithelial cancers, including esophageal, gastric, lung, head, neck and Merkel cell cancers (Sozzi *et al*., 1996). About 50% of these tumors display aberrant *FHIT* gene transcripts, which lack exons that are considered relevant for the normal function of that encoded protein. While the Choi-CK cells displayed an aberrantly migrating *FHIT* transcript, the SCK cells showed the both the aberrant and normal transcripts. Therefore, this aberrant *FHIT* transcript does not seem to be relevant to the histological degree of differentiation. A tumor evasion mechanism involving Fas/FasL exists in intrahepatic cholangiocarcinoma and the downregulation of Fas and FasL was correlated with histologic dedifferentiation and invasion (Que *et al*., 1999; Shimonishi *et al*., 2000). In this study, all four CC cell lines showed variable expressions of *Fas/FasL* mRNA, with no correlation to the histological grade of differentiation. However, the SCK cells expressed lower levels of *Fas/FasL* mRNA than did the ordinary CC cells.

EMT is triggered by oncogenic activation and the primary mode of EMT induction is provided by specific growth factors or extracellular matrix components binding to their cognate cellular receptors. Hepatocyte growth factor and its receptor, Met tyrosine kinase, is one of the predominant modulators of EMT that has been described to date (Birchmeier *et al*., 1996). Activation of intrinsic kinase activity by their cognate ligands initiates a cascade of cytoplasmic events. This specific transduction pathway involved in EMT consists of Src involvement or the Ras pathway (Boyer *et al*., 1997). Several transcriptional activators are capable of controlling the EMT process. For example, Fos induces an EMT process by activating a Wnt-like pathway, which is initiated by β-catenin nuclearization (Eger *et al*., 2000). Other transcription factors, including the snail family and another snail family slug and the Ets family, are also

candidates for playing a role in EMT during embryonic life and they may also participate in tumor progression (Batlle *et al*., 2000). However, the molecular mechanism of EMT whereby tumor cells acquire the phenotype of invasiveness and metastasis is still unclear. Thus, the establishment of sarcomatoid CC cell lines and their genetic analysis may provide us with new information about EMT and the progression of CC.

Vimentin positive cancer cells seem to undergo an EMT event whereby the markers of epithelial differentiation are reduced or even lost and a vimentin expression is acquired (Hendrix *et al*., 1997). VIM alone was recently shown not to be sufficient to confer the invasive metastatic phenotype (Hendrix *et al*., 1997). Wnt glycoproteins have been implicated in EMT and also in the diverse processes during embryonic patterning in metazoa. They signal through frizzled-type seven-transmembrane-domain receptors to stabilize β-catenin. Wnt signaling is antagonized by the extracellular Wnt inhibitor DKK1 (Wu *et al*., 2000). Unexpectedly, the over-expression of *DKK1* was found in SCK cells. Thus, its role should be further clarified. Up-regulation of lactate dehydrogenase (LDH) ensures an efficient anaerobic/glycolytic metabolism for tumor cells and reduces dependence on oxygen (Koukourakis *et al*., 2005). Expressions of mammalian LDHA and LDHB are regulated tissue-specifically during individual development, thus the alterations in serum LD isoenzyme pattern could serve as indicators of pathological involvement and cancer development. The levels of LDHB were specifically elevated in lung cancer patients and progressively increased with the clinical stage of non-small cell lung cancer (Chen *et al*., 2006). The expression of UCHL1 is closely associated with the advanced stages of lung cancer and with the invasive colorectal cancer (Hibi *et al*., 1999; Yamazaki *et al*., 2002). Consistently, our data showed that the upregulations of LDHB and UCHL1 were closely correlated with CC dedifferentiation.

Non-sarcomatous Choi-CK cells express more cytoskeletal structure genes than do sarcomatous SCK cells. The cholangiocarcinoma specific antigens *KRT7* and *KRT19* were preferentially expressed in the Choi-CK cells, which was consistent with the previous immunohistochemical findings (Wu *et al*., 1996). Cell growth-related genes, including *EGFR*, *BST2*, *CCND*, and *AREG*, are also over-expressed in these cells. The EGFR expression has been believed to contribute to the tumor progression of CC (Ito *et al*., 2001). However, the SCK cells expressed less EGFR than did the other carcinomatous CC cells, and so the dedifferentiation seems to rather be associated with the down-regulation of EGFR. ANXA8 is a calcium-dependent phospholipid-binding protein that was previously identified as a blood anticoagulant, based on *in vitro* studies, and it may have a role in the signal transduction pathway in acute promyelocytic leukemia cells (Sarkar *et al*., 1994). The present results showed that the ANXA8 expression was down-regulated in SCK cells. The expressions of S100P and GPX1 were also decreased according to CC dedifferentiation.

In the recent studies of various cancers, expression arrays have provided insights that were difficult to obtain when single genes or pathways were studied in the past. In the present study, the microarray data was in accordance with the results from both the Northern blotting analysis and the immunohistochemistry. Thus, we recognized the sarcomatous change/EMT-related gene expression profile in CC cells with the sarcomatous phenotype. Some of this data confirmed previous knowledge whereas some of the other data is novel. Some of these novel genes may show promise as clinical markers that are significantly up- or down-regulated in sarcomatoid or carcinomatous CC, and they may prove to be additional targets for new strategies to effectively treat cancer.

Methods

Cell cultures, tumorigenicity and histopathological examination

Four CC cell lines were grown in DMEM supplemented with 10% FBS and 1% antibiotics-antimycotics in a 5% CO_2 air conditioned (37°C) incubator as described previously (Kim *et al*., 2001). Four- to six-week old female BALB/c nude mice were purchased from the animal breeding laboratory at Korea Research Institute of Bioscience and Biotechnology (Daejeon, Korea). All mice were group-housed under conditions of constant light cycle (12 h light/12 h dark) and fed *ad libitum* access to sterilized food and water. The animal protocols used were approved by the Institutional animal Care and Use Committee of Chonbuk National University Hospital. To confirm their tumorigenicities and morphological characteristics, the four human CC cell lines (SCK, JCK1, Cho-CK and Choi CK) were xenografted to 4- to 6-week-old female athymic nude mice. The JCK1 cells were derived from the original JCK cells and morphologically worse differentiated than the original cells. The cells ($0.5\text{-}1 \times 10^7$) in 0.2 ml culture medium were injected subcutaneously into the flanks of mice. When the subcutaneous tumors reached a diameter of 1 cm or more, the mice were sacrificed. The subcutaneous tumors were then processed for light microscopy and they were subcultured. The tumors that arose from the xenografts were excised, fixed in 10% formaldehyde solution and embedded in paraffin for histological examination.

The sections were stained with hematoxylin and eosin. Immunohistochemistries for differentially expressed genes were performed in the xenotransplanted masses of all four SCK, JCK, Cho-CK, and Choi-CK cells. The endogenous peroxidase activity was blocked with using methanol/hydrogen peroxide, and after this the tumor tissues were stained by an avidin-biotin-complex immunoperoxidase method with using a commercially available kit (Vector, Burlingame, CA) and antibodies that recognized vimentin (VIM), carcinoembryonic antigen (CEA), alpha- fetoprotein (AFP), albumin, fibrinogen, epithelial membrane antigen (EMA) or epithelial keratin (KRT7, KRT19 and KRT20) (Dako, Copenhagen, Denmark). The immunoperoxidase reaction was then developed with aminoethylcarbazole (Sigma, St. Louis, MO).

Detection of *p53* mutations

Four regions of the p53 gene were amplified from genomic DNA extracts with p53-specific primers. The genomic DNA was extracted and mixed with 10 *p*mole/μl of forward and reverse primers, buffer and *Taq* polymerase (2.5 U, Takara, Shiga, Japan). The conditions of PCR were 30 cycles of amplification through denaturation at 95°C for 1 min, annealing at an appropriate temperature (59-69°C) for 30 s and then extension at 72°C for the proper time, respectively. For cDNA sequencing, one μg of total RNA was reverse-transcribed with the random decamers of a Retroscript kit (Ambion, Austin, TX). PCR of the cDNA was performed as described above. Direct sequencing was performed by the dideoxy chain termination reaction according to the manufacturer's method. The primers for genomic and cDNA sequencing are described in Supplemental Data Table S1.

Detection of the *FHIT* gene expression

The total RNA was extracted from the cells with using Tri Reagent (Molecular Research Center Inc. Cincinnati, OH) and following the manufacturer's instructions. The mRNA was reverse transcribed with oligo d(T)15 primers (Boehringer Mannheim, Mannheim, Germany) to prepare single-stranded cDNA. Two different PCR assays were used to assess the status of the *FHIT* gene transcript (Supplemental Data Table S1). The first was based on the previously reported nested PCR approach (Ohta *et al*., 1996). Using the 5U2 primer, the 3D2 primer, 100 μM of each dNTP, 10× PCR polymerase mix and 1 unit Advantage *Taq* polymerase (Clontech, Palo Alto, CA), the PCR reaction was cycled 25 times in a Perkin-Elmer thermal cycler (model 9700). One μl of a 20-fold dilution was then used in a subsequent nested PCR assay with using the primers 5U1 and 3D1. Analysis of the *FHIT* gene transcript was repeated with using another set of primers MUR5 and RP23 (Thiagalingam *et al*., 1996). The primer MUR5 partially overlaps the primer 5U1 in exon 3, and the primer RP2 partially overlaps primer 3D2 in exon 10. The PCR products were electrophoresed on 2% agarose gels (FMC Bioproducts, Rockland, ME).

Fas and FasL mRNA expression

The mRNA was reverse transcribed with using oligo d(T)15 primers (Boehringer Mannheim) to prepare the single-stranded cDNA, and this was followed by PCR amplification of the *Fas* mRNA or the *FasL* mRNA. Amplification was performed for 30 cycles for β-actin as an internal control and for *Fas* in a thermal cycler (Perkin Elmer). Each cycle consisted of 1 min of denaturation at 94°C, 1 min of annealing at 57°C and 1 min of extension at 72°C. The sequences of primers used were as follows, *Fas* (forward: 5'CGGAGGATTGCTAACAAC3', reverse: 5'TTGGTATTCTGGGTCCG3') (Panayiotidis *et al*., 1995) and *β-actin* (forward: 5'CGTTCTGGCGGCACCACCAT3', reverse: 5'GCAACTAAGTCATAGTCCGC3') (Wong *et al*., 1994). *FasL* RT-PCR amplification was done for 35 cycles. The sequences of the *Fas-L* primers are: forward 5'CAAGTCCAACTCAAGGTCCAT3' (nt 610-630, NM_000639.1) and reverse 5'AACGTATCTGAGCTCTCTCTG3' (nt 935-955) (Mita *et al*., 1994). The PCR conditions consisted of 1 min of denaturation at 94°C, 1 min of annealing at 55°C and 1 min of extension at 72°C. The PCR products were analyzed by electrophoresis on 1.2% agarose gels.

Northern blot analysis

5×10^6 cells were harvested by treatment of Trypsin-EDTA and they were washed in cold PBS. The total RNA was isolated using an Rneasy mini kit (Qiagen) according to the manufacturer's protocol. The total RNA, a 20 μg/sample, was separated on 1% agarose gels in 1.8 M formaldehyde and then the RNA was transferred to membranes. The blots were hybridized overnight with a 2×10^6 cpm/ml cDNA probe labeled with [^{32}P]dCTP (NEN, Boston, MA) by randompriming; the blots were washed and then exposed to x-ray film at -70°C, as described previously (Yu *et al*., 2007). The expressed levels of each gene were calculated by normalizing them against the level of *18S* rRNA.

Cell lysis and immunoblotting

The cells were lysed in a buffer containing 50 mM Tris-HCl (pH 8.0), 150 mM NaCl, 1% Triton X-100, 5 mM EDTA, 5 mM ethylene glycol-bis (β-aminoethyl ether) N,N,N',N'-tetraacetic acid, 10 mM NaF, 1 mM Na_3VO_4, 1 mM PMSF, 2 μg/ml leupeptin, 1 mM pepstatin and 1 μg/ml aprotinin. Thirty μg of each cell lysate was separated by SDS-PAGE and this was was transferred to Hybond membranes (Amersham Pharmacia Biotech, Uppsala, Sweden). The membranes were blocked with 5% skim milk and they were then incubated with the designated primary antibodies, and the signals were detected using an ECL Western blotting kit (Amersham Pharmacia Biotech). Mouse anti-p53 (DO-1) monoclonal and rabbit p21 (C-19) polyclonal antibodies were purchased from Santa Cruz Biotechnology, Inc. (Santa Cruz, CA).

Preparation of the florescence-labeled cDNA and the microarray hybridization

The two sets of cDNA microarrays (14k and 4.6k) used in this study were made by 21C Frontier the Center for Functional Analysis of Human Genome (Korea Research Institute of Bioscience and Biotechnology, Daejon, Korea)

and Macrogen, Ltd. (Seoul, Korea). The fluorescence-labeled cDNA probes were made from 100 μg of total RNA for each tumor cell line by oligo(dT)-primed polymerization with using SuperScript II reverse transcriptase (Invitrogen Co., Carlsbad, CA). The reaction was carried out in a final volume of 50 μl as described previously (Yu *et al*., 2007). Fluorescent nucleotides Cy5- dUTP and Cy3-dUTP (Amersham) were used at 0.2 mM. The nucleotide concentrations were 1 mM for the dGTP, dATP and dCTP and 0.4 mM dTTP. Two hundred units of Superscript II was added at the beginning of the labeling reaction that was incubated at 42°C. Two hundred units more were added after 1 h and the reaction was continued for a further 1 h. The Cy5 and Cy3 probes were mixed and the probe volume was reduced to 30 μl using a Microcon 30 (Millipore, Bedford, MA). The purified and concentrated fluorescence-labeled cDNAs from the experimental samples were boiled for 5 min, and a hybridization mixture was prepared in a final volume of 100 μl that contained blocking reagents in sodium saline citrate (SSC)/SDS solution and was mounted on the microarray slides. After placing a coverslip on the slide, hybridization was performed at 65°C for 15 h in a hybridization cassette (TeleChem, Sunnyvale, CA). The slides were washed with 1× SSC / 0.1% SDS for 15 min at 55°C twice and with 0.1× SSC/0.1% SDS for 15 min at 55°C twice, and then they were washed again in 0.1× SSC for 10 min at room temperature. The slides were dried by a brief spin at 500 rpm for 1 min and then they were immediately subjected to image processing.

Imaging and image analysis

The fluorescence intensities generated by the Cy5 or Cy3 immobilized at the target sequence on the microarray slides were measured by a laser confocal microscope scanning system ScanArray 4000XL (GSI Lumonics, Billerica MA). The two fluorescent images (Cy5 and Cy3) were scanned separately and they were stored for further image analysis. The color images were generated by arbitrarily assigning experimental intensity values into the red channel and the reference intensity values into the green channel and *vice versa*. The signals from each immobilized cDNA target on a microarray slide were localized and the expression ratio between the experimental samples and the reference (the Cy5/Cy3 ratio) was determined with using ImaGene 4.2 (BioDiscovery, Los Angeles, CA). The fluorescence intensities of Cy5 and Cy3 for each target spot were adjusted so that the median Cy5 and Cy3 intensities of all the spots for each slide were equal. The entire hybridization experiments and image analysis were repeated after swapping dyes.

Data analysis

To assess the correlation of the intensity value for each cDNA between the sarcomatoid CC cells and the non-sarcomatoid CC cells, scatter plots were used and a linear relationship was measured in log space. To determine the significance of the gene expression changes, we used the Significance Analysis of Microarray (SAM) method (Tusher *et al*., 2001). Briefly, the SAM method computes a score for each gene that measures the difference of the mean log-ratio from zero with using modified one-sample *t*-statistics. The false discovery rate (FDR) was calculated from the order statistics obtained by randomly multiplying the log-ratios by +1 or -1 with equal probability. The Δ value, which sets the minimum difference between observed and expected scores, was set to 0.76, resulting in a median FDR of 2.0%. The list of genes was further filtered by selecting those genes that showed at least a 4-fold change.

Supplemental Data

Supplemental Data include a Table and can be found with this article online at http://e-emm.or.kr/article/article_files/SP-41-2-06. pdf.

Acknowledgments

This work was supported by grants from the Korea Health 21 R&D Project (A050328), Ministry of Health and Welfare, the 21C Frontier Human Genome Project grant (FG08-12-03), Ministry of Science and Technology of Korea, the Program for Cancer Control from the Ministry of Health, Welfare and Family affairs (0620220), and the Research Institute of Clinical Medicine, Chonbuk National University Hospital, Republic of Korea. This work was also supported by a grand to K.Y. Choi from the National R&D program for Cancer Control, Ministry of Health, Welfare and Family affairs, Republic of Korea (0620200-1).

References

Ahrendt SA, Nakeeb A, Pitt HA. Cholangiocarcinoma. Clin Liver Dis 2001;5:191-21

Batlle E, Sancho E, Francí C, Domínguez D, Monfar M, Baulida J, García De Herreros A. The transcription factor snail is a repressor of E-cadherin gene expression in epithelial tumour cells. Nat Cell Biol 2000;2:84-9

Birchmeier C, Birchmeier W, Brand-Saberi B. Epithelial-mesenchymal transitions in cancer progression. Acta Anat (Basel) 1996;156:217-26

Boyer B, Roche S, Denoyelle M, Thiery JP. Src and Ras are involved in separate pathways in epithelial cell scattering. EMBO J 1997;16:5904-13

Chang WW, Agha FP, Morgan WS. Primary sarcoma of the liver in the adult. Cancer 1983;51:1510-7

Chen Y, Zhang H, Xu A, Li N, Liu J, Liu C, Lv D, Wu S, Huang L, Yang S, He D, Xiao X. Elevation of serum l-lactate dehydrogenase B correlated with the clinical stage of lung cancer. Lung Cancer 2006;54:95-102

D'Errico A, Baccarini P, Fiorentino M, Ceccarelli C, Bonazzi C, Ponzetto A, Scoazec JY, Mancini AM, Grigioni WF. Histogenesis of primary liver carcinomas: strengths and weaknesses of cytokeratin profile and albumin mRNA detection. Hum Pathol 1996;27:599-604

Eger A, Stockinger A, Schaffhauser B, Beug H, Foisner R. Epithelial mesenchymal transition by c-Fos estrogen re-

ceptor activation involves nuclear translocation of beta-catenin and upregulation of beta-catenin/lymphoid enhancer binding factor-1 transcriptional activity. J Cell Biol 2000; 148:173-88

Goodman ZD, Ishak KG, Langloss JM, Sesterhenn IA, Rabin L. Combined hepatocellular-cholangiocarcinoma. A histologic and immunohistochemical study. Cancer 1985;55: 124-35

Hendrix MJ, Seftor EA, Seftor RE, Trevor KT. Experimental co-expression of vimentin and keratin intermediate filaments in human breast cancer cells results in phenotypic interconversion and increased invasive behavior. Am J Pathol 1997;150:483-95

Hibi K, Westra WH, Borges M, Goodman S, Sidransky D, Jen J. PGP9.5 as a candidate tumor marker for non-small-cell lung cancer. Am J Pathol 1999;155:711-5

Ito Y, Takeda T, Sasaki Y, Sakon M, Yamada T, Ishiguro S, Imaoka S, Tsujimoto M, Higashiyama S, Monden M, Matsuura N. Expression and clinical significance of the erbB family in intrahepatic cholangiocellular carcinoma. Pathol Res Pract 2001;197:95-100

Kakizoe S, Kojiro M, Nakashima T. Hepatocellular carcinoma with sarcomatous change. Clinicopathologic and immunohistochemical studies of 14 autopsy cases. Cancer 1987; 59:310-6

Kim DG, Park SY, You KR, Lee GB, Kim H, Moon WS, Chun YH, Park SH. Establishment and characterization of chromosomal aberrations in human cholangiocarcinoma cell lines by cross-species color banding. Genes Chromosomes Cancer 2001;30:48-56

Levine AJ. The p53 tumor-suppressor gene. N Engl J Med 1992;326:1350-2

Mita E, Hayashi N, Iio S, Takehara T, Hijioka T, Kasahara A, Fusamoto H, Kamada T. Role of Fas ligand in apoptosis induced by hepatitis C virus infection. Biochem Biophys Res Commun 1994;204:468-74

Oda Y, Katsuda S, Nakanishi I. An autopsy case of hepatic sarcomatoid tumor: immunohistochemical comparison with a sarcomatous component of hepatocellular carcinoma. Pathol Int 1994;44:230-6

Ohta M, Inoue H, Cotticelli MG, Kastury K, Baffa R, Palazzo J, Siprashvili Z, Mori M, McCue P, Druck T, Croce CM, Huebner K. The FHIT gene, spanning the chromosome 3p14.2 fragile site and renal carcinoma-associated t(3;8) breakpoint, is abnormal in digestive tract cancers. Cell 1996;84:587-97

Panayiotidis P, Ganeshaguru K, Foroni L, Hoffbrand AV. Expression and function of the FAS antigen in B chronic lymphocytic leukemia and hairy cell leukemia. Leukemia 1995;9:1227-32

Que FG, Phan VA, Phan VH, Celli A, Batts K, LaRusso NF, Gores GJ. Cholangiocarcinomas express Fas ligand and disable the Fas receptor. Hepatology 1999;30:1398-404

Sarkar A, Yang P, Fan YH, Mu ZM, Hauptmann R, Adolf GR, Stass SA, Chang KS. Regulation of the expression of annexin VIII in acute promyelocytic leukemia. Blood 1994;84:279-86

Savagner P, Yamada KM, Thiery JP. The zinc-finger protein slug causes desmosome dissociation, an initial and necessary step for growth factor-induced epithelial-mesenchymal transition. J Cell Biol 1997;137:1403-19

Shimonishi T, Isse K, Shibata F, Aburatani I, Tsuneyama K, Sabit H, Harada K, Miyazaki K, Nakanuma Y. Up-regulation of fas ligand at early stages and down-regulation of Fas at progressed stages of intrahepatic cholangiocarcinoma reflect evasion from immune surveillance. Hepatology 2000;32:761-9

Sozzi G, Alder H, Tornielli S, Corletto V, Baffa R, Veronese ML, Negrini M, Pilotti S, Pierotti MA, Huebner K, Croce CM. Aberrant FHIT transcripts in Merkel cell carcinoma. Cancer Res 1996;56:2472-4

Thiagalingam S, Lisitsyn NA, Hamaguchi M, Wigler MH, Willson JK, Markowitz SD, Leach FS, Kinzler KW, Vogelstein B. Evaluation of the FHIT gene in colorectal cancers. Cancer Res 1996;56:2936-9

Tusher VG, Tibshirani R, Chu G. Significance analysis of microarrays applied to the ionizing radiation response. Proc Natl Acad Sci USA 2001;98:5116-21

Wong H, Anderson WD, Cheng T, Riabowol KT. Monitoring mRNA expression by polymerase chain reaction: the "primer-dropping" method. Anal Biochem 1994;223:251-8

Wu PC, Fang JW, Lau VK, Lai CL, Lo CK, Lau JY. Classification of hepatocellular carcinoma according to hepatocellular and biliary differentiation markers. Clinical and biological implications. Am J Pathol 1996;149:1167-75

Wu W, Glinka A, Delius H, Niehrs C. Mutual antagonism between dickkopf1 and dickkopf2 regulates Wnt/beta-catenin signalling. Curr Biol 2000;10:1611-4

Yamazaki T, Hibi K, Takase T, Tezel E, Nakayama H, Kasai Y, Ito K, Akiyama S, Nagasaka T, Nakao A. PGP9.5 as a marker for invasive colorectal cancer. Clin Cancer Res 2002;8:192-5

You KR, Shin MN, Park RK, Lee SO, Kim DG. Activation of caspase-8 during N-(4-hydroxyphenyl)retinamide-induced apoptosis in Fas-defective hepatoma cells. Hepatology 2001;34:1119-27